

Measurement of the anisotropic electron-phonon scattering rates in Al

T. Wegehaupt* and R. E. Doezema

Physik-Department, Technische Universität München, D-8046 Garching, Federal Republic of Germany

(Received 27 March 1978)

From the linewidths of resonant transitions between surface Landau levels, we extract electron-phonon scattering rates at 13 Fermi-surface locations in Al. In the temperature range 2–10 K we find that the scattering rate varies by more than a factor of 10 over the Fermi surface, the highest rates being found near the Brillouin-zone boundaries. The observed scattering rates are compared with two recent theoretical calculations. Deviations are found, but the overall trend in the anisotropy is well predicted by both calculations. The present experiment does not confirm predicted departures from the usual T^3 scattering law.

I. INTRODUCTION

Two recent calculations^{1,2} have predicted the variation of the electron-phonon scattering rates³ over the Fermi surface (FS) of Al. Here we present a detailed⁴ experimental study of the thermal scattering at a number of locations on the Al FS in the temperature range 2–10 K. The scattering rates are extracted from the linewidths of microwave resonances between surface Landau levels.⁵ Surface-Landau-level resonance (SLLR) is a method ideally suited for studying anisotropic scattering because the electron states contributing to the resonance lines are localized to small, well-defined regions on the FS.

A full study of the SLLR spectra in three sample planes in Al, together with the resulting variation of the anisotropic mass-enhancement parameter over the FS, has been reported in a separate paper.⁶ In the present work, we rely on the assignments made there, which relate the resonances to FS locations. Additional details, such as temperature control and measurement, are to be found in a similar study for Cu.⁷

The magnetic surface levels correspond classically to electrons skipping along a smooth sample surface under the influence of a weak magnetic field \vec{H} applied in the sample plane. The resonances are observed as changes in the surface impedance of the metal, with resonance field given by

$$H_{mn} = \frac{c\hbar}{e} \left(\frac{\omega}{a_n - a_m} \right)^{3/2} \left(\frac{2K}{v_F^3} \right)^{1/2}. \quad (1)$$

Here ω is the microwave frequency and the a_n ($n = 1, 2, \dots$) are the zeros of the Airy functions. Peaks in the field derivative of the surface resistance dR/dH , occur near the resonance condition (1) and originate from those electrons on the FS "effective zone" (\vec{v}_F parallel to sample surface), where $(K/v_F^3)_\perp$ is extremal with respect to the k -space coordinate k_H along the magnetic field. The symbol \perp denotes the component in the plane per-

pendicular to the magnetic field direction. If the FS geometry, i.e., the FS curvature radius K is accurately known, one thus obtains⁶ the Fermi velocity v_F from the observed field values of the resonances.

The widths of the dR/dH peaks are related to the electronic scattering rates. From the relative width at half amplitude $\Delta H/H$ for the 1–2 transition we measure the scattering rate Γ by⁷

$$\Gamma = (\omega/1.56)(\Delta H/H - 0.02). \quad (2)$$

For each point \vec{k} on the FS the total scattering rate is composed of a temperature-independent and a temperature-dependent part

$$\Gamma(\vec{k}) = \Gamma_0(\vec{k}) + \Gamma(\vec{k}, T). \quad (3)$$

We concentrate in this paper on the anisotropy of the temperature-dependent part of the scattering rate. The temperature-independent part, due to impurities, defects, and possibly some surface scattering, is also expected to be anisotropic. Very recently, the anisotropy of Γ_0 due to quench- and irradiation-induced defects has been investigated⁸ for Al using the SLLR method. The large anisotropy of $\Gamma(\vec{k}, T)$ over the FS is immediately apparent in Fig. 1, where a surface state spectrum containing resonances from three locations on the FS is shown for two sample temperatures.

Although the extraction of scattering rates from the SLLR line shape has been discussed in previous publications,^{6,9,10} we briefly review the relevant concepts before turning to a discussion of our Al data. We shall pay particular attention to the various averages involved in making up the resonance line. This will be important in discussing the deviations, predicted by theory,^{1,2} from the simple T^3 power law for the scattering rate usually expected in the low-temperature regime.^{10,11} The line-shape averages are also important in relating the measured rates to theoretically calculated quasiparticle scattering rates.

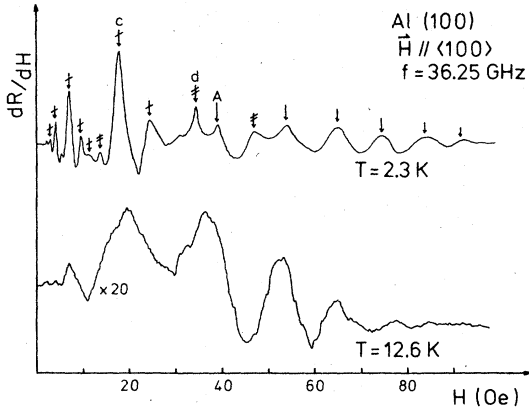


FIG. 1. Temperature evolution of a surface state spectrum containing signals from three Fermi surface locations. The 1 \rightarrow 2 transitions are indicated by letters and subsidiary transitions are marked accordingly. The belly series A has the lowest electron-phonon scattering rate and, in contrast to the 2.3-K trace, dominates the spectrum at 12.6 K.

II. DEFINING THE MEASURED SCATTERING RATE

Stated in simplest terms, the measured scattering rate is a fitting parameter which relates the experimental line-shape to the theoretical line-shape expression. The aim of this section is to sketch some of the important concepts involved in the interpretation of the scattering parameter and to discuss in detail two interpretational aspects which, in the case of SLLR, have not been adequately discussed up till now.

The resonant part of the line-shape function dR/dH is an energy integral of the form⁵

$$\int_{-\infty}^{\infty} \left(-\frac{\partial f}{\partial \epsilon} \right) \frac{d\epsilon}{\omega - \omega_{mn} + i/\tau_0}, \quad (4)$$

where f is the Fermi function, τ_0 is the lifetime parameter, and ω_{mn} is the resonance frequency obtained from (1) by making the replacements $H_{mn} \rightarrow H$ and $\omega \rightarrow \omega_{mn}$. The electrons which contribute to the dR/dH peaks which result from (4) are to be found on a strip⁹ about the point on the FS where ω_{mn} is extremal. The width of the strip is of the order $10^{-2}k_F$ and its length $10^{-1}k_F$, where k_F is the Fermi wave vector.

Scattering events are effective if the scattering wave vector is large enough to remove the electron from the strip, i.e., to destroy its resonance. For the case of phonons in Al, the arguments of Ref. 9 may be applied to show that the scattering is effective in the temperature range of interest in this paper. We need not, therefore, weight scattering events according to effectiveness—such weighting would lead to an increase in the exponent of the power-law dependence of the scatter-

ing rate.¹¹

An additional cause of change in the scattering power law is the “ k_H broadening.” This refers to the contribution of electrons in the neighborhood of the extremal point to the line shape. It has been argued⁹ that for $\omega\tau \gtrsim 5$ this effect can be neglected, and therefore we limit our results to this range. Although not responsible for an altered power law, the “ k_H broadening” does affect the value of the measured scattering rate: it represents an averaged value over the length of the k_H strip. Using the variation of $(K/v_F^3)_L^{1/2}$ about the extremal point, one can estimate⁹ the strip length over which the measured scattering rate applies.

In the remainder of this section we first discuss the effect of the electron-phonon renormalization on the measured value of the scattering rate and then estimate the effect of the thermal smearing of the FS on the measured SLLR scattering rate.

A. Electron-phonon renormalization

At temperatures low compared with the Debye temperature Θ_D and for excitation energy ϵ (measured from the Fermi energy) small compared to $k_B\Theta_D$, the electron-phonon interaction¹² increases the particle mass over the band mass m_B according to $m^* = m_B(1 + \lambda)$. The mass-enhancement parameter is related to the real part of the quasiparticle self-energy M_{SE} by $\lambda = -\partial M_{SE}/\partial \epsilon$. The imaginary part of the self-energy Γ_{SE} produces the quasiparticle scattering rate: $1/\tau_{qp} = 2\Gamma_{SE}/\hbar$.

We now ask how the expression (4) is to be interpreted in the presence of the electron-phonon interaction. The result parallels that of Goy and Castaing¹³ for Azbel'-Kaner cyclotron resonance. They in turn made use of the theoretical results of Scher and Holstein.¹⁴ When the interaction is turned on, the resonant denominator in (4) is replaced by

$$\omega(1 + \lambda) - \omega_{mn} + i/\tau, \quad (5)$$

where τ now includes the temperature- and energy-dependent scattering due to the electron-phonon interaction

$$1/\tau = 1/\tau_0 + 1/\tau_{qp}. \quad (6)$$

If we wish to regain the form of (4), with which the line-shape analysis is performed, we must rewrite (4) as

$$\int_{-\infty}^{\infty} \left(-\frac{\partial f}{\partial \epsilon} \right) \frac{d\epsilon}{\omega - \omega_{mn}^* + i/\tau^*}. \quad (7)$$

(For Al we may safely neglect the energy and temperature dependence of λ since $\Theta_D \gg T$, $\hbar\omega/k_B$.) Experimentally, therefore, one observes a renor-

malized resonant frequency

$$\omega_{mn}^* = \omega_{mn} / (1 + \lambda), \quad (8)$$

and a renormalized scattering rate,

$$\Gamma = \frac{1}{\tau^*} = \frac{1}{(1 + \lambda)} \left(\frac{1}{\tau_0} + \frac{1}{\tau_{qp}} \right). \quad (9)$$

Measurement of ω_{mn}^* gives the (renormalized) Fermi velocity at various points \vec{k} on the FS a known FS geometry. If the band velocity $v_F^B(\vec{k})$ is known, one then obtains $\lambda(\vec{k})$ from $v_F(\vec{k}) = v_F^B(\vec{k}) [1 + \lambda(\vec{k})]^{-1}$. In a previous publication⁶ values of $\lambda(\vec{k})$ for Al were extracted from the surface-state resonances.

The quasiparticle scattering rate is given according to Eq. (9) by the observed scattering rate $\Gamma(\vec{k})$ multiplied by the factor $1 + \lambda(\vec{k})$. This is a generally applicable result: Goy and Castaing¹³ find it for cyclotron resonance and Wampler and Lengeler¹⁵ have recently given a clear discussion for the de Haas-van Alphen effect.

The previous neglect⁷ of the factor $1 + \lambda$ in comparing theoretical and experimental scattering rates in Cu is not too serious, since λ is of the order of 0.1 for Cu. In Al, however, λ is of the order of 0.5 and we shall therefore include the correction when comparing to theory.

B. Energy averaging

The electron-phonon scattering rate takes on a minimum value of the FS. Away from the FS the rate increases with excitation energy ϵ above or below the FS (where we take $\epsilon = 0$). Thus in any real experiment, the thermal smearing of the FS causes a larger rate to be measured than the rate on the FS. In the Debye approximation, the simple energy average of the electron-phonon scattering rate $\Gamma(T, \epsilon)$ is given by¹⁶

$$\langle \Gamma(T, \epsilon) \rangle = \int_{-\infty}^{\infty} \left(-\frac{\partial f}{\partial \epsilon} \right) \Gamma(T, \epsilon) d\epsilon = \frac{12}{7} \Gamma(T, 0). \quad (10)$$

The way in which $\Gamma(T, \epsilon)$ is actually averaged in a given experiment is usually not so simple and depends on the experimental line-shape function, i.e., not all $\Gamma(T, \epsilon)$ values are to be weighted equally as in the average (10) above. Allen¹⁷ has pointed out the intimate connection between the energy averaged Γ and the line-shape function for Azbel'-Kaner cyclotron resonance; and Wagner and Albers¹⁶ have discussed the energy averaging in detail for the case of the radio-frequency size effect. We wish here to illustrate the expected effect of energy averaging on the electron-phonon scattering rate measured in SLLR.

The energy integral to be performed is given by expression (7). The experimental line shape is

analyzed with the Prange-Nee theory, as if there were an averaged scattering rate $\bar{\Gamma}$ such that

$$\frac{1}{\omega - \omega_{mn}^* + i\bar{\Gamma}} = \int_{-\infty}^{\infty} \left(-\frac{\partial f}{\partial \epsilon} \right) \frac{d\epsilon}{\omega - \omega_{mn}^* + i\Gamma(\epsilon)}. \quad (11)$$

The total energy-dependent scattering rate $\Gamma(\epsilon)$ is assumed to be composed of the usual two terms:

$$\Gamma(\epsilon) = \Gamma_0 + \Gamma(T, \epsilon). \quad (12)$$

For $\Gamma(T, \epsilon) \ll \Gamma_0$, we expand both sides of (11) and find that the averaged rate is given approximately by Eq. (10). This comes about because the line-shape weighting in this limit comes from the constant Γ_0 .

In the opposite limit, $\Gamma(T, \epsilon) \gg \Gamma_0$, we expand both sides of (11) again to find

$$\langle \Gamma(T, \epsilon) \rangle \approx \frac{\int_{-\infty}^{\infty} (-\partial f / \partial \epsilon) (1 / \Gamma(T, \epsilon)) d\epsilon}{\int_{-\infty}^{\infty} (-\partial f / \partial \epsilon) [1 / \Gamma(T, \epsilon)]^2 d\epsilon}. \quad (13)$$

This is the same result found by Goy and Castaing¹⁸ for cyclotron resonance. The crossover point between the two limits occurs near $\langle \Gamma(T, \epsilon) \rangle \approx \frac{5}{3} \Gamma_0$, a condition which is usually satisfied in the experimental temperature range. It is therefore important to ask whether the averaging expressed in (13) gives a substantially different result than Eq. (10).

We have numerically performed the integrations of Eq. (13) using the expansion¹⁶

$$\Gamma(T, \epsilon) \cong \Gamma(T, 0) \left[1 + \frac{1}{2} \alpha (\epsilon / k_B T)^2 \right]. \quad (14)$$

With the correct value for $\alpha = 0.33$ we obtain $\langle \Gamma(T, \epsilon) \rangle \approx 1.21 \Gamma(T, 0)$, which is substantially different from Eq. (10). Increasing¹⁶ the value of α to simulate the effect of higher-order terms in the expansion (14) does not alter this conclusion [$\alpha = 0.6$ yields $\langle \Gamma(T, \epsilon) \rangle = 1.28 \Gamma(T, 0)$]. Thus for a fixed power law of scattering, $\Gamma(T, 0) = \gamma T^n$, one expects to measure a lower averaged value of γ at the higher temperatures, where $\Gamma_0 < \Gamma(T)$ compared to the very low temperature regime. Such a decrease in γ could conceivably be misinterpreted as a decreased power-law exponent.

III. EXPERIMENTAL RESULTS

In this section we present our measured scattering rates as a function of sample temperature. The rates are extracted in the usual way⁷ from the line-widths of the various 1-2 transitions at 36 GHz using Eq. (2).

In Fig. 2 the resulting scattering rates for four characteristic points on the FS are plotted against T^3 . The locations of the points on the FS are given in Table I and result from the identifications made in Ref. 6. Due to the large number of signals in

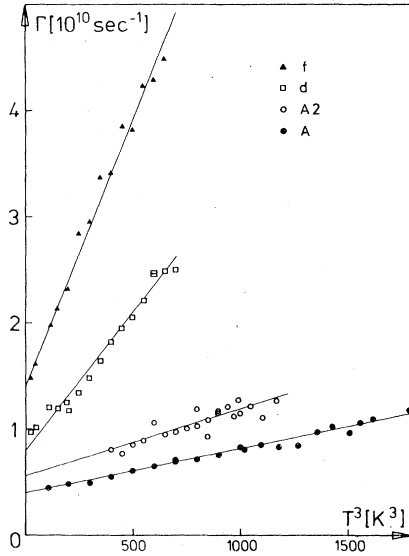


FIG. 2. Measured scattering rates vs T^3 for four FS locations.

Al, it is not always possible to completely isolate a given 1-2 transition and thus avoid "artificially" distorting the extracted scattering rate by superimposed peaks. Although we attempt to correct for such distortions, peaks distorted in this way generally lead to the large scatter in data points, seen for two of the locations in Fig. 2. Such distortions also tend to limit the range of temperatures over which the scattering rate can be measured. Thus relatively large error bars must be assigned to the measured rate of increase with T^3 of the scattering for such locations.

Within the accuracy of the present measurements, we are not able to demonstrate departures from the usual T^3 scattering law. We therefore analyze the data according to

$$\Gamma(\vec{k}) = \Gamma_0(\vec{k}) + \gamma(\vec{k})T^3. \quad (15)$$

The slope $\gamma(\vec{k})$ is then a measure of the strength of the anisotropic electron-phonon scattering, and within its stated accuracy predicts the electron-phonon scattering rate through (15) at any temper-

TABLE I. Comparison between experimental and theoretical electron-phonon scattering rates in Al. Listed are the location angle ϕ in the extended zone scheme; the measured scattering-rate slope versus T^3 , $\gamma(\vec{k})$; the temperature range over which these values apply; and the experimental slopes adjusted for energy averaging and renormalization. The two values given for each theoretical calculation refer, respectively, to the 5-K and 10-K rates. These rates apply at the Fermi surface and should be compared to the adjusted experimental rates.

Point	ϕ (deg) ^a	$\gamma(\vec{k})$ ($10^7 \text{ sec}^{-1}/\text{K}^3$)	ΔT (K)	$\frac{7}{12} [1 + \lambda(\vec{k})] \gamma(\vec{k})^b$ ($10^7 \text{ sec}^{-1}/\text{K}^3$)	$T^{-3}/\tau_{qp}(E_F, T)$ Ref. 1	($10^7 \text{ sec}^{-1}/\text{K}^3$) Ref. 2
A	0	0.41 ± 0.03	4-13	0.34 ± 0.025	0.20-0.22	0.23-0.23
A1 ^c	10.9	0.78 ± 0.16	4-10	0.66 ± 0.13	0.27-0.33	...
A2	-7.8	0.63 ± 0.14	7-11	0.53 ± 0.12	0.24-0.27	...
A3	-11.4	1.2 ± 0.3	4-11	1.0 ± 0.3	0.33-0.36	...
B	51.3	0.39 ± 0.03	4-13	0.31 ± 0.025	0.09-0.18	0.22-0.22
B1	67.0	0.54 ± 0.05	4-11	0.44 ± 0.04
B2	81.3	0.71 ± 0.09	4-12	0.63 ± 0.08
B3	40.5	0.35 ± 0.04	4-13	0.29 ± 0.03	0.18-0.23	0.22-0.22
B4	37.0	1.2 ± 0.3	4-10	1.0 ± 0.3	0.24-0.38	0.3-0.4
c	17.0	3.5 ± 0.2^d (3.1 ± 0.3)	2-9	3.0 ± 0.2 (2.6 ± 0.25)	1.3-2.2	2.7-2.9
d	-36.0	2.6 ± 0.3	3-9	2.2 ± 0.3	0.8-1.7	...
e	30.5	1.5 ± 0.7	2-5	1.4 ± 0.7	3.2-2.3	2.9-2.2
f	87.1	5.0 ± 0.5	2-8	3.9 ± 0.4	...	3.0-3.3

^a Measured from the zone center with respect to the $\langle 100 \rangle$ direction; positive values refer to the $\{110\}$ plane and negative values to the $\{100\}$ plane.

^b $\lambda(\vec{k})$ values from Ref. 6.

^c Close to point A1 of Ref. 6.

^d Measured in the (100) plane; value in parentheses measured in the (110) plane.

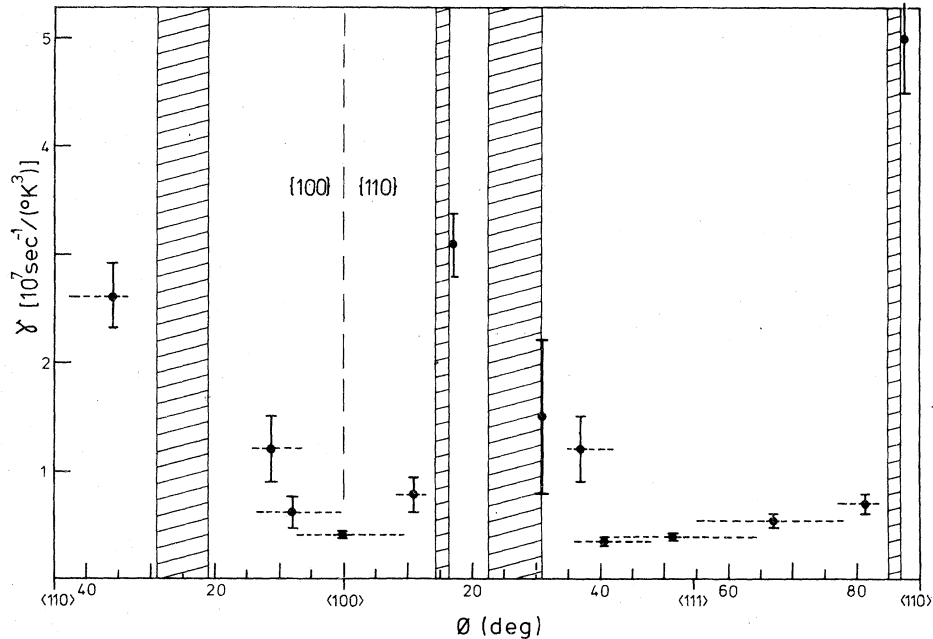


FIG. 3. Measured T^3 coefficient of the scattering rate at various locations on the central $\{100\}$ and $\{110\}$ Fermi-surface slices. The angle ϕ denotes location in the extended zone scheme as measured with respect to the $\langle 100 \rangle$ axis. Dashed lines indicated the region of Fermi surface over which the measured rate represents an average. The three points without dashed lines are averaged over a length normal to the indicated plane.

ature within the measured range of temperatures (Table I). The impurity and defect scattering rate $\Gamma_0(\vec{k})$ is also seen from Fig. 2 to be anisotropic, but does not vary by much more than a factor of 2. It is found to be generally higher for the third-zone arm portions of the FS than for the free-electron-like belly portions in the present samples.

Our results for $\gamma(\vec{k})$ are summarized in Fig. 3. The locations of the various FS points are again indicated in Fig. 4 for clarity. The dashed widths in Fig. 3 refer to the length of the FS strip for which the indicated rates represent averaged values. The length of the strip for each location may be simply estimated from the linewidth and known $(K/v_F)_\perp$ variation of the corresponding resonance.⁹

IV. DISCUSSION AND CONCLUSIONS

It is evident from Fig. 3 that the electron-phonon scattering rates in Al are quite anisotropic. They rise by more than a factor of 10 from the low-belly values to the high rates on ridge and arm sections near the Brillouin-zone boundaries. Much of the anisotropy can be accounted for by the increased coupling of electrons with transverse phonons near the zone boundaries.² In Table I we have made a comparison with the theoretical predictions for the scattering rates. In the table we have adjusted the experimental values for the $\frac{7}{12}$ factor expected from the thermal averaging (at

least at the lowest temperatures) and for the factor $1 + \lambda(\vec{k})$ from renormalization. [The experimental $\lambda(\vec{k})$ values are taken from our work in Ref. 6.] The observed anisotropy is well predicted by the theoretical calculations, although the observed scattering rates on the belly portions are considerably higher than the calculated rates.

The ratios of the theoretical scattering rates to T^3 are listed in Table I for the temperatures 5 and 10 K, which span our experimental range. Variation between the ratio values at the two tempera-

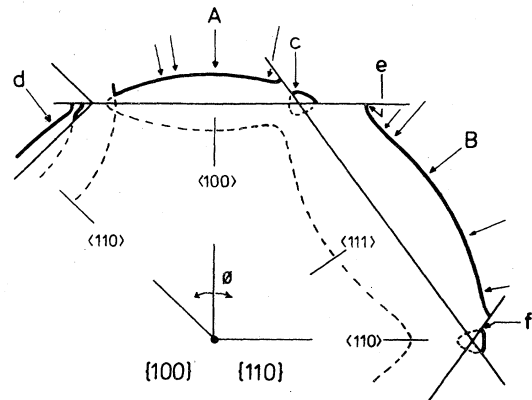


FIG. 4. Locations on the $\{100\}$ and $\{110\}$ central planes of the Al Fermi surface where the scattering rates have been measured.

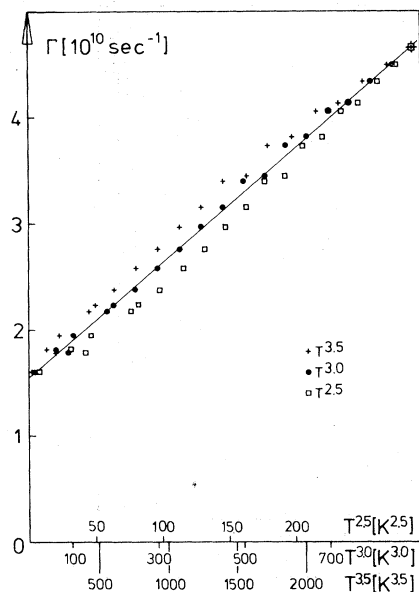


FIG. 5. Scattering rates for point *c* in the (100) sample plane plotted against $T^{2.5}$, T^3 , and $T^{3.5}$. The solid line represents the best fit for the T^3 relation.

tures are indicative of the predicted breakdown of the T^3 relation. Reasons for the breakdown have been discussed by Meador and Lawrence² and by Leung *et al.*¹⁹ Examination of the uncertainties associated with the experimental scattering rates together with the spread in theoretical values over our temperature range, shows for most of the FS points that the present experimental results are incapable of confirming the predicted T^3 departures. Few of our FS locations show the T^3 relation as unambiguously as does point *c* in Fig. 5. It is, however, clear that the strong T^3 deviation predicted in Ref. 1 for the

point *B* is ruled out by the experiment. In connection with deviations on the second zone, it should also be pointed out that, for the central (110) orbit of Fig. 4, a strict T^3 relation has been observed in the radio-frequency size effect.²⁰ A final comment concerning the predicted T^3 departures is that after the averaging along the FS strip is taken into account, the deviations may no longer be so severe. [Much the same is found to occur for the (110) arm cyclotron resonance orbit.²¹]

Perhaps it is more remarkable that the reduction in the measured scattering rate increase with T^3 —of the order of 30%—which we predicted because of energy averaging in Sec. II, is not observed. Nor for that matter was it observed in Cu.⁷ We have no explanation for this. Maybe it is a result of incomplete knowledge of the scattering rate away from the Fermi energy, or, alternatively, due to an incomplete understanding of the SLLR line shape.

The present experiment has thus pointed out certain remaining difficulties in the theoretical description of the electron-phonon scattering in Al, and in the interpretation of the SLLR line shape. On the other hand, the power of the method in measuring the anisotropy of the scattering has once again been convincingly demonstrated.

ACKNOWLEDGMENTS

We wish to express our appreciation to J. F. Koch for his encouragement throughout the course of this project. We thank W. Mohr and J. S. Lass for critical comments and pleasant discussions. We also wish to thank H. D. Drew, W. E. Lawrence, and R. E. Prange for valuable communication. Financial support was provided by the Bundesministerium für Forschung und Technologie.

*Present address: Sektion Physik, Ludwig-Maximilians-Universität München, D-8000 München, F.R.G.

¹P. G. Tomlinson and J. P. Carbotte, *Solid State Commun.* **18**, 119 (1976).

²A. B. Meador and W. E. Lawrence, *Phys. Rev. B* **15**, 1850 (1977).

³For recent reviews, see, V. F. Gantmakher, *Rep. Prog. Phys.* **37**, 317 (1974); J. F. Koch and R. E. Doezema, *Proceedings of the Fourteenth International Conference on Low Temperature Physics, 1975* (American Elsevier, New York, 1975), Vol. 5, p. 314.

⁴Preliminary results were reported in, R. E. Doezema and T. Wegehaupt, *Solid State Commun.* **17**, 631 (1975).

⁵R. E. Prange and T. W. Nee, *Phys. Rev.* **168**, 779 (1968); T. W. Nee, J. F. Koch, and R. E. Prange, *ibid.* **174**, 758 (1968).

⁶T. Wegehaupt and R. E. Doezema, *Phys. Rev. B* **16**,

2515 (1977).

⁷R. E. Doezema and J. F. Koch, *Phys. Rev. B* **6**, 2071 (1972).

⁸W. Mohr and J. S. Lass (unpublished).

⁹R. E. Doezema and J. F. Koch, *Phys. Condens. Mat.* **19**, 17 (1975).

¹⁰J. F. Koch and R. E. Doezema in Ref. 3.

¹¹See, e.g., N. W. Ashcroft and N. D. Mermin, *Solid State Physics* (Holt, Rinehart and Winston, New York, 1976), p. 525.

¹²For a recent review, see G. Grimvall, *Phys. Scr.* **14**, 63 (1976).

¹³P. Goy and B. Castaing, *Phys. Rev. B* **7**, 4409 (1973); **11**, 2696 (1974).

¹⁴J. Scher and T. Holstein, *Phys. Rev.* **148**, 598 (1966).

¹⁵W. R. Wampler and B. Lengeler, *Phys. Rev. B* **15**, 4614 (1977).

¹⁶D. K. Wagner and R. C. Albers, *J. Low Temp. Phys.* 20, 593 (1975).

¹⁷P. B. Allen, *Proceedings of the Twelfth International Conference on Low Temperature Physics, 1970* (Academic, Japan, 1971), p. 517.

¹⁸P. Goy and B. Castaing, *Phys. Rev. B* 11, 2696 (1975).

¹⁹H. K. Leung, J. P. Carbotte, D. W. Taylor, and C. R. Leavens, *Can. J. Phys.* 54, 1585 (1976).

²⁰V. A. Gasparov and M. H. Harutunian, *Solid State Commun.* 19, 189 (1976).